(Preprint) AAS 13-226

ON THE NATURE OF EARTH-MARS PORKCHOP PLOTS

Ryan C. Woolley[*] and Charles W. Whetsel[†]

Porkchop plots are a quick and convenient tool to help mission designers plan ballistic trajectories between two bodies. Parameter contours give rise to the familiar "porkchop" shape. Each synodic period the pattern repeats, but not exactly, primarily due to differences in inclination and non-zero eccentricity. In this paper we examine the morphological features of Earth-to-Mars porkchop plots and the orbital characteristics that create them. These results are compared to idealistic and optimized transfers. Conclusions are drawn about "good" opportunities versus "bad" opportunities for different mission applications.

INTRODUCTION

Plotting interplanetary trajectory parameters such as C_3 and V_∞ in launch-date/arrival-date space and tracing isometric lines are a valuable mission design tool that are used in optimizing the trajectories for most interplanetary missions. The most important energy parameters (C_3 and V_∞) typically create bi-lobed characteristic shapes which have earned these plots the colloquial nickname of "porkchop" plots. Porkchop plots aide early mission designers in selecting launch dates, in calculating launch energies and ΔV budgets, and visually optimizing trajectories. Launch periods are designed by applying constraints on some parameters (e.g. launch declination, arrival dates, launch period duration, entry speed, sun angles) while simultaneously minimizing others (e.g. launch energy, Mars orbit insertion (MOI) ΔV).[1,2,3]

Each opportunity (~26 months for Earth to Mars) a new porkchop plot is created with similar characteristics, but with different minima (on either side of the central ridge), minima locations, ridge width, and lobe shapes. In this paper we investigate how the orbital characteristics of Earth and Mars affect the nature of the porkchop plots and how they compare to ideal (circular, coplanar) and optimized (allowing launch, arrival, and transfer time to be free parameters) porkchop plots. We also explore what defines a "good" opportunity for Mars missions and to what extent certain characteristics repeat with Mars cycles (approximately 15 years or 7 opportunities) and super-cycles.

PORKCHOP PLOTS

Lambert's Theorem can be used to calculate the orbital parameters of the trajectory between any two points for a given time of flight (TOF).[4] This means that for any launch date at Earth

[*] Systems Engineer, Pre-Projects Systems Engineering Group, Jet Propulsion Laboratory, California Institute of Technology, 4800 Oak Grove Drive, Pasadena, CA 91109.
[†] Manager, Mars Advanced Studies and Program Architecture Office, Jet Propulsion Laboratory.
2013 California Institute of Technology. Government sponsorship acknowledged.

(which specifies location 1) and arrival date at Mars (which specifies location 2 and TOF), there exists a conic trajectory connecting the two. Plotting contours of the relevant parameters of the connecting trajectories against combinations of launch date and arrival date create a two-lobed chart known as a porkchop plot. While traditional porkchop plots often portray the specific departure energy and hyperbolic excess arrival energy individually (C_3 and V_∞ respectively), for the purposes of this investigation, the authors chose to focus on a combination of these parameters, termed the "total transfer ΔV". Figure 1 shows total transfer ΔV (defined in Equation 1, below) for the 2018 Earth-to-Mars opportunity.

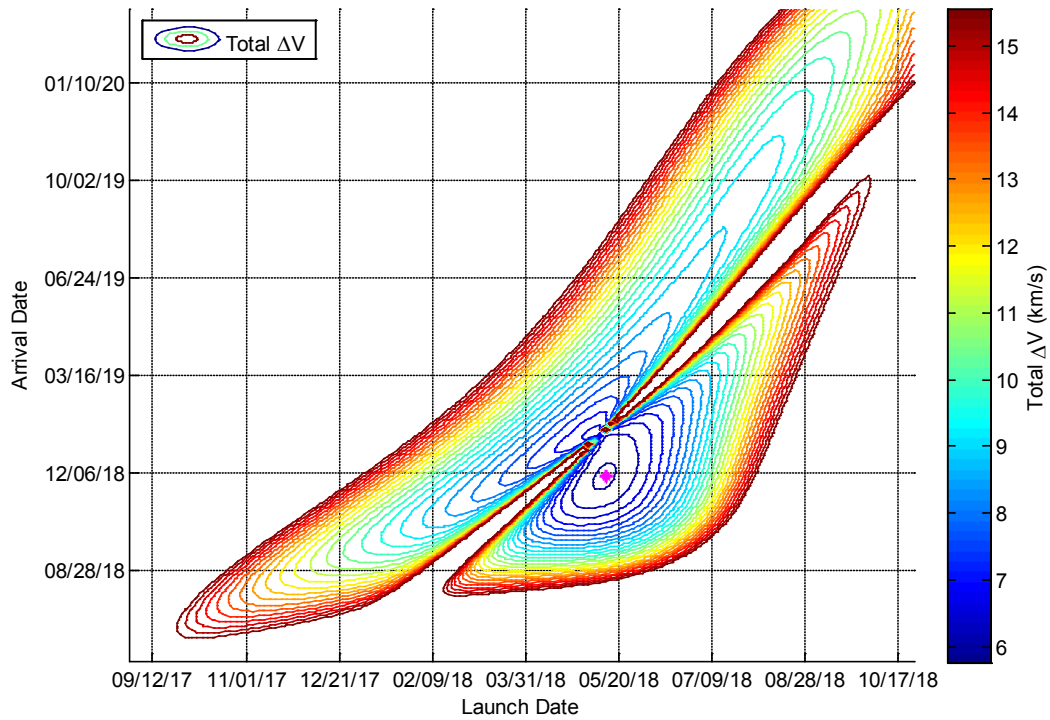

Figure 1. 2018 Earth-to-Mars Porkchop Plot with total ΔV contours.

Trajectories below the central ridge are referred to as Type I trajectories (< 180°), and trajectories above are Type II's (>180°). The ridge itself is due to the fact that Earth and Mars do not lie in the same plane. Hohmann-like transfers, therefore, generally necessitate a large out-of-plane component which in turn requires a large amount of energy, creating the ridge. When Earth and Mars are phased properly the trajectory remains in-plane and a "bridge" is formed across that central ridge.

Over a larger range of departure and arrival dates we can see that the minima are repeated each synodic period, as shown in Figure 2. A closer examination of each opportunity reveals that the lobed structure varies in size and shape, as do the central ridge width and locations (Type I vs. II) and values of the minimum ΔV trajectory. Since the Earth goes around the sun 2.14 times each synodic period, the relative geometry of Earth and Mars shifts by 48.7 degrees.[5]

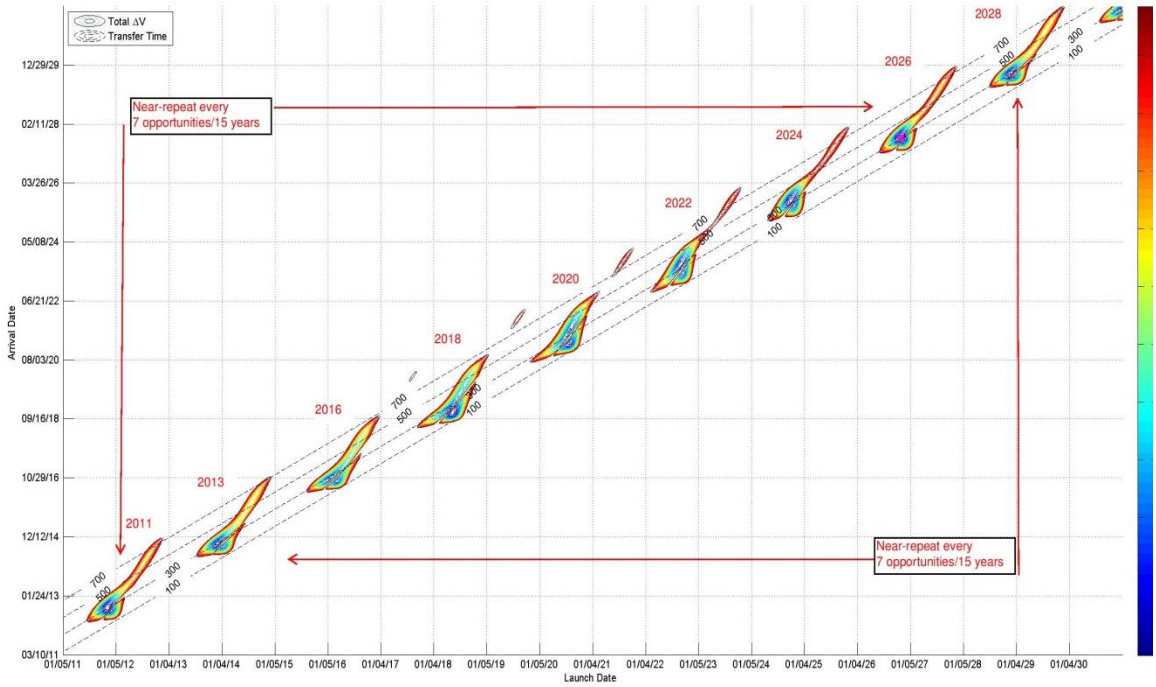

Figure 2. Multiple porkchop plots from 2011-2028 showing changing shape and structure. Each date on the *x* and *y* axes corresponds to perihelion for Earth and Mars, respectively. Note the location of the minimum ΔV for each opportunity with respect to the squares on the grid. Every 7 opportunities the minima are in a similar location resulting in a near-repeat.

OPTIMIZED PORKCHOP PLOTS AND TRANSFERS

In order to compare the quality of trajectories from one opportunity to the next, it is necessary to choose a figure-of-merit (FOM). This simplifies matters by allowing us to plot one set of contours and to define optimal trajectories. The choice of a FOM is subjective and can be defined by mission objectives. For our purposes we chose to use the total transfer ΔV as defined by

$$\Delta V = \left|V_{Earth}(t_1) - V_T(t_1)\right| + \left|V_{Mars}(t_2) - V_T(t_2)\right| \tag{1}$$

where t_1 is the time at launch, t_2 is the time at arrival, and V_T is the velocity of the transfer trajectory. This is the orbital transfer equation (neglecting gravity at Earth and Mars) and was chosen because it balances the contributions of C_3 and V_∞.

Since Mars is inclined 1.85° to the ecliptic and both Earth and Mars have non-zero eccentricities, true Hohmann transfers are not possible. The actual ephemerides of the planets constrain the transfer angles and times when other parameters are chosen. If we let launch location (true anomaly of Earth, ν_{Earth}), arrival location (true anomaly of Mars, ν_{Mars}), and transfer time (Δt) be free variables it is possible to find the ΔV optimized trajectory for each ν_{Earth}-ν_{Mars} pair. Plotting the contours of minimized ΔV vs. ν_{Earth} and ν_{Mars} (as opposed to launch date/arrival date) creates an "optimized porkchop plot" that is that is strictly a function of departure and arrival geometry for Earth and Mars, and is decoupled from time (i.e. makes no assumption about in which real years or which real launch/arrival opportunities these specific geometric conditions exist).

Earth-Mars Transfer Geometry

The shape and characteristics of Earth-Mars porkchop plots are driven by the relative geometry and dynamics between their heliocentric orbits. Semimajor axes drive the synodic period, transfer time, and ΔV requirements whereas eccentricity, inclination, and perihelion locations refine the characteristics that shape each individual opportunity. It is instructive to begin with the basic case of circular orbits and add in each of the orbital elements in order to observe the effects of each.

Case 1: Circular Co-Planar. If Earth and Mars were in circular, co-planar orbits the optimal ΔV transfer would be a Hohmann transfer with launch and arrival separated by 180° and a total ΔV of 5.59 km/s (see Table 1 for other parameters). This optimal transfer would be available once per synodic period (779.94 days) and shorter or longer transfers would be possible at the expense of additional ΔV. Transfer trajectories from any point along Earth's orbit to any point along Mars' orbit are shown in the optimized porkchop plot in Figure 3b. Transfer time was allowed to vary from 200 to 350 days.

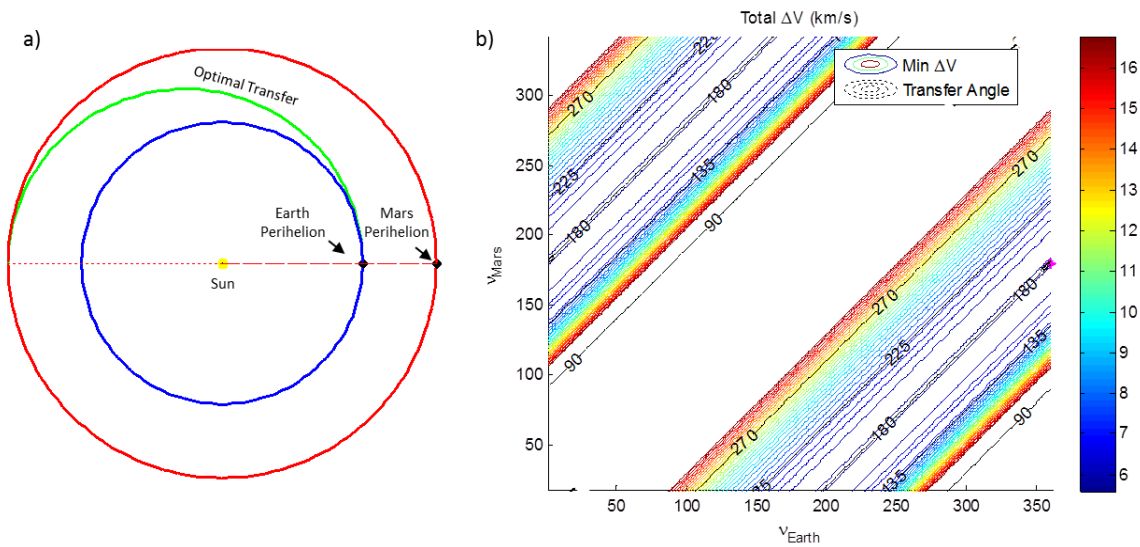

Figure 3. Case 1 - Hohmann Transfer in Earth-Mars Circular Co-Planar Model. a) Heliocentric view of Earth-Mars orbits with 180° Hohmann transfer. b) Optimized Porkchop Plot for this case. Colored contours depict minimum transfer ΔV for each true anomaly (ν) pair and black lines show the transfer angle. Transfer angles of 180° result in the minimum Hohmann ΔV of 5.59 km/s.

Case 2: Adding Eccentricity. Earth has an eccentricity of 0.0167 while Mars is more eccentric at 0.0934. If the perihelia were aligned, 180° transfers starting at perihelion and ending at aphelion would still be optimal.[6] The most ΔV efficient trajectory starts at Earth perihelion and ends at Mars aphelion, shown in Figure 4a, with a total ΔV of 5.49 km/s – 0.1 km/s less than that of a circular Hohmann. This is because it is more fuel efficient to raise apoapsis while moving quickly at periapsis, and to raise periapsis while moving slowly at apoapsis. In effect, this can be thought of as creating a range of preferable departure geometries near ν_{Earth} = 0° (a region with "near-perihelion departure advantages") as well as a range of preferable arrival geometries near ν_{Mars} =180° (a region with "near-aphelion arrivals advantages").

Note that the lines of constant ΔV are no longer strictly parallel with the transfer angle lines, suggesting that departures/arrivals from some locations are preferable to others. For Earth departures from perihelion to aphelion (0°-180°) and Mars arrivals from 180° - 360°, trajectories with transfer angles greater than 180° (Type II) result in lower total ΔV's. With the departure/arrival conditions reversed, Type I trajectories are favored. The worst transfer in this case is for the 180° transfer originating at Earth aphelion (ΔV = 5.58 km/s).

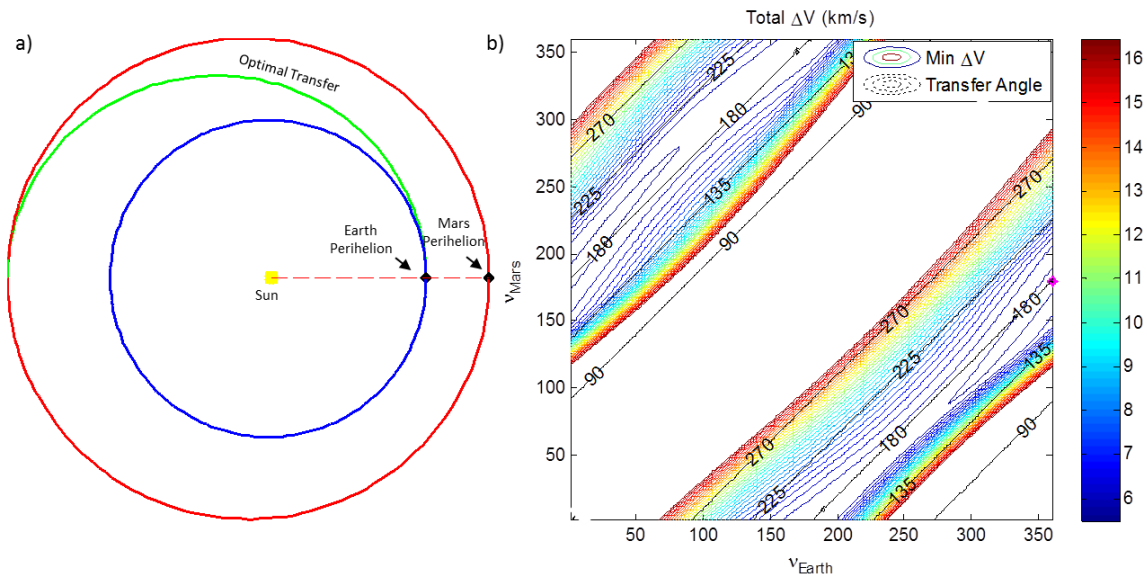

Figure 4. Case 2 - Transfers Between Eccentric, Co-planar Orbits with Collocated Apsides. a) The lowest ΔV transfer leaves from Earth perihelion and arrives at Mars aphelion. Total ΔV = 5.49 km/s. b) The optimized porkchop plot shows that non-180° transfers are optimal except at the apsides (i.e. the bottom of the "contour valley" does not coincide with the 180° transfer line). The magenta diamond represents the optimal transfer.

Case 3: Rotating the Lines of Apsides (Co-planar). The actual perihelia of Earth and Mars are separated by 127°, which we will call Γ (shown in Figure 5a). The addition of offset perihelia disallows the possibility of an efficient transfer which takes advantage of perihelion departure and aphelion arrival (because the apsides of the two orbits are no longer aligned). Since Mars' orbit is almost six times more eccentric than that of Earth's, the ΔV benefit of arriving near aphelion far outweighs that of leaving near perihelion. The optimal transfer is a 186° Type II trajectory that arrives 10° past Mars' aphelion (ν_{Mars} = 190°), but leaves Earth at a true anomaly of 236.4° (far from Earth perihelion). The shift away from Earth perihelion adds 17 m/s the total ΔV and 19 days to the transfer. A closer inspection of the contour lines in Figure 5b shows that the lowest contour spans a wide range of departure and arrival space. For an additional 100 m/s it is possible to arrive at Mars at true anomalies of 150-230°. For this case it Type I trajectories are optimal for Earth departures between 44° and 244° whereas Type II's are optimal over the other region, including the global minimum.

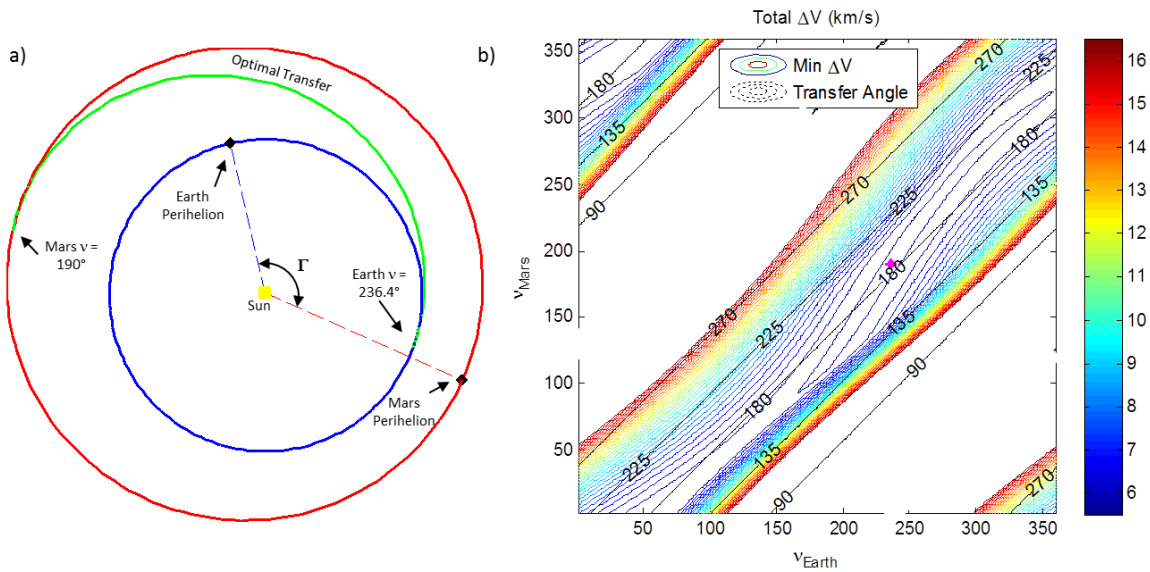

Figure 5. Case 3 - Transfers Between Eccentric, Co-planar Orbits with Offset Apsides. Earth and Mars are offset by Γ = 127°. a) The optimal trajectory arrives near Mars aphelion. Total ΔV = 5.51 km/s. b) The optimal porkchop plot is more influenced by Mars' location than Earth's due to its greater eccentricity. This is evident from the lowest contour being drawn towards Mars aphelion. The magenta diamond represents the optimal transfer.

Case 4: Circular Inclined. If the orbits* are re-circularized and the inclination of Mars (1.85°) is considered, interesting features arise. The optimized porkchop plot in Figure 6b now has a ridge along the 180° transfer line. 180° transfers have very high heliocentric inclinations which require prohibitively large ΔV's of 20-75 km/s. However, this plot also exhibits two "bridges" along that ridge where low energy transfers are possible. These two points occur at the ascending and descending nodes of Mars' orbit and the corresponding locations along Earth's orbit. They are located at (ν_{Earth} = 127°, ν_{Mars} =74°) and (ν_{Earth} = 307°, ν_{Mars} =254°).

There are two identical optimal transfers in the circular case that start and end along the line of nodes (see Figure 6a) – through the "bridges in the ridge". They are very similar to the planar Hohmann case except that each burn is a combined maneuver to change the inclination by 0.87° at Earth and by 0.98° at Mars (sum total of 1.85°, the inclination of Mars' orbit w.r.t the ecliptic). The uneven split in inclination change is due the fact that it is less costly to change inclination at slower velocities at Mars arrival. The combined maneuvers add an additional 70 m/s to the total ΔV (to 5.66 km/s).

While it is possible to perform transfers when Mars is out of the ecliptic, they will generally require up to 1-2 km/s more than transfers originating near the line of nodes. These are the Type I and Type II trajectories found in the "troughs" on either side of the central ridge. Type I's are more advantageous for Earth departures from 127° to 217° and 307° to 37°, whereas Type II's are lower in the other regions.

* The periapsis offset, Γ, is still used here, but has no bearing on the results as periapsis is undefined for a circular orbit. It was desirable to retain the relationship between periapses and the ascending node so as to better illustrate the effects of inclination in the Earth-Mars system and to provide a common coordinate system with the prior figures in this paper.

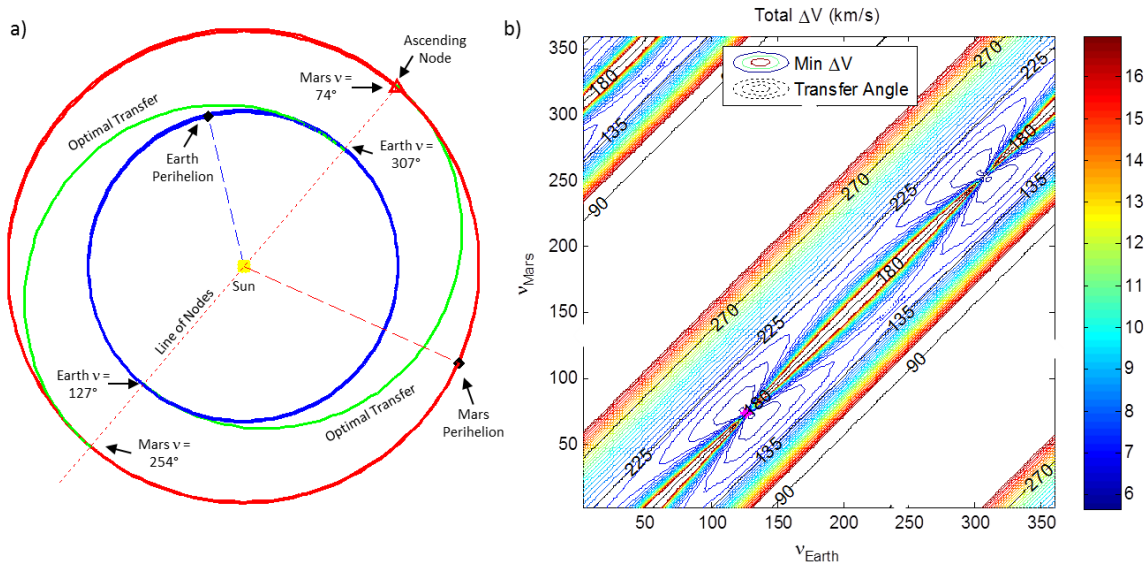

Figure 6. Case 4 - Transfers Between Circular Inclined Orbits. a) The lowest ΔV transfers start and end at the line of nodes. Total ΔV = 5.66 km/s. b) The optimal porkchop plot now has "ridges" and "bridges" and is symmetric about the 180° transfer line. The bridges indicate the location of the line of nodes and are the optimal transfers in this case.

Case 5: Actual Earth-Mars Model. The combination of the true eccentricity, apsidal offset, and inclination result in the optimized porkchop plot shown in Figure 7b. It represents the lower bounding surface for actual opportunities, which are constrained by the true ephemerides of Earth and Mars to have a prescribed Δt for any two locations (or, conversely, a prescribed arrival location for a given departure location and Δt). Each ν_{Earth}-ν_{Mars} pair on the optimized porkchop plot has its own transfer time optimized for minimal ΔV, which are shown in Figure 8b. In theory,

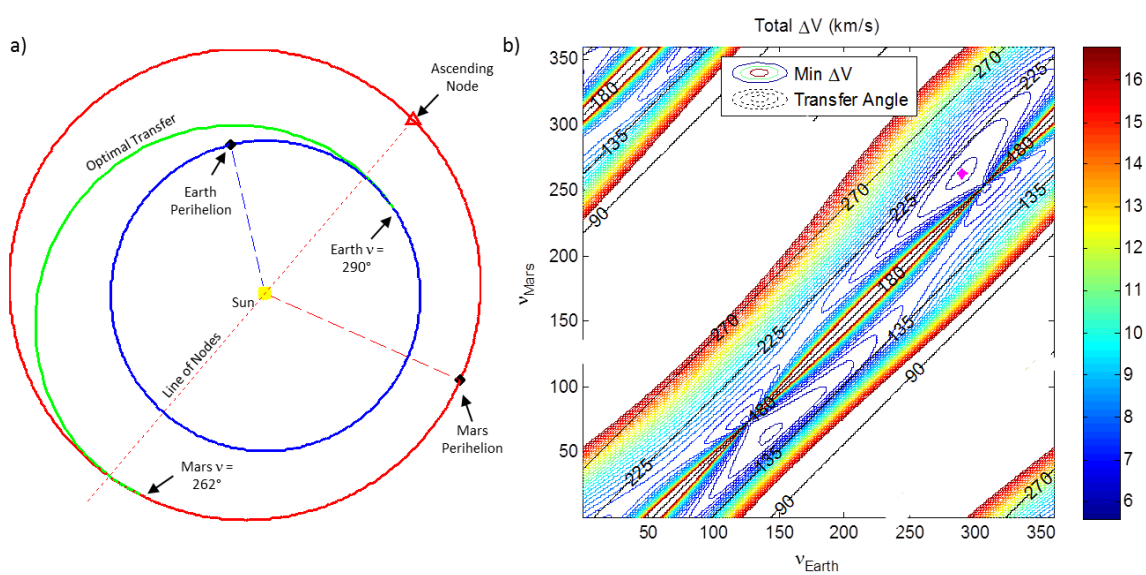

Figure 7. Case 5 - Optimized Earth-Mars Trajectories. Minimum ΔV with transfer time as a free parameter. a) The global optimal transfer is a Type II trajectory that starts and ends near the line of nodes. Total ΔV = 5.60 km/s. b)

each optimal condition will occur eventually, but it may require thousands of years. The precise geometry of the absolute minimum will not occur until the year 8368, although in 2073 and 2162 it comes quite close. The global optimum transfer leaves Earth in the fall (ν_{Earth}=290° corresponds to mid-October), about 15° before crossing Mars' line of nodes. It arrives 313 days later in late August just after (6°) Mars has descended through the ecliptic. Optimal ΔV trajectories for actual opportunities are discussed in the next section.

If we look at a 3D view of the optimized porkchop plot (see Figure 8a) we note the existence of two low troughs or valleys on either side of the abrupt 180° transfer ridge. Further away from the ridge transfer trajectories are possible, but at the cost of 10's of km/s in ΔV. These trajectories would also require long (>350 days) or short (<180 days) flight times as shown in Figure 8b. Although the absolute minimum is a Type II* trajectory that occurs near one of the bridges†, there are reasonably low ΔV (<7.5 km/s) trajectories available for departures at any Earth true anomaly. In fact, the minimum ΔV Type I trajectory, located by the other bridge, occurs at (ν_{Earth}=143°, ν_{Mars}=64°) and is just 30 m/s higher than the Type II at 5.63 km/s.

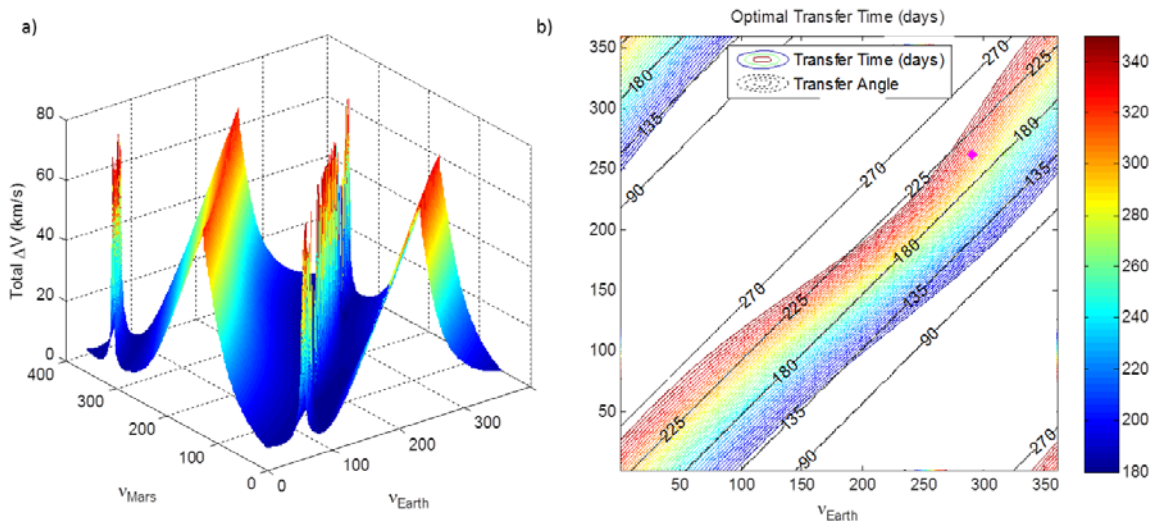

Figure 8. a) 3-Dimensional view of optimal porkchop plot with ridges and valleys. b) Optimized transfer times associated with Figure 7b. Transfer times longer or shorter than these for any given ν–ν pair are possible, but at the cost of higher ΔV's than those show on the optimal porkchop plot.

Table 1 below summarizes the results from the optimized transfers from Cases 1-5. In terms of total ΔV, we can see that adding eccentricity decreases the amount needed by ~100 m/s whereas inclination requires combined maneuvers raise it by a similar amount. Once the apsides are offset the end result is a total optimal transfer ΔV quite similar to that of a Hohmann. The main difference, however, is that the transfer angle has increased by 25° and the transfer duration by ~50 days. The right two columns show the best and worst of optimized trajectories over 2011-2043. 2026 comes quite close to the global optimum whereas 2016 requires about 30% more fuel.

---

* Type II trajectories are located in the "left valley" above the 180° ridge whereas Type I's are located below it.
† Note that he bridges in the full model are in the same locations as Case 4.

Table 1. ΔV Optimized Earth-Mars Transfers

Parameter	Case 1 **Circular Co-planar**	Case 2 **Eccentric Co-planar**	Case 3 **Rotated Apsides**	Case 4 **Circular Inclined**	Case 5 **Full Model**	Actuals (2011-2043) **Best (2026)**	**Worst (2016)**
Total ΔV (km/s)	5.59	5.49	5.51	5.66	5.60	5.61	7.12
ΔV_1 (km/s)	2.94	3.40	3.57	2.98	3.06	3.04	3.36
ΔV_2 (km/s)	2.65	2.09	1.94	2.68	2.54	2.57	3.76
Transfer Angle	180°	180°	187°	180°	205.3°	205.7°	214.1°
Transfer Time	259 days	278 days	293 days	259 days	313 days	311 days	277 days
Launch (ν_{Earth})	n/a	0°	236.4°	306.7°	290.2°	294.2°	13.1°
Arrival (ν_{Mars})	n/a	180°	190°	253.5°	262.3°	266.8°	354.6°
Eccentricity	0.208	0.258	0.245	0.208	0.221	0.218	0.176

ANALYSIS

This research was carried out using Earth and Mars true anomaly as a coordinate frame for departures and arrival so that it would be readily apparent how close transfers occur to the apsides. Earth true anomaly can also be used as a surrogate for day of the year since Earth perihelion typically occurs around January 4 and 365 days is close to 360°. Mars true anomaly is not as enlightening, other than to indicate where Mars is with respect to its apsides. Once we note that Mars line of nodes occurs at ν_{Mars} = 74° and 254° it is easier to see why the most fuel-efficient trajectories cluster there. Also of interest to mission designers is the Mars season at arrival, measured by the solar longitude, or L_s. Mars L_s starts at 0° at its vernal equinox in the same way that Earth's vernal equinox starts at the 1st point of Aries – both being related to axial tilt orientation. The 1st point of Ares is the point of reference for most heliocentric reference frames. It may be useful to convert the locations presented in this paper into one of these alternate frames of reference. For this purpose Table 2 is included with the appropriate conversion factors.

Table 2 - Heliocentric Longitudinal Reference Frames and Conversions

Measurement Frame	Reference Point	Convert From: **Heliocentric**	**Earth ν**	**Mars ν**	**Mars L_s**
Heliocentric (Earth L_s)	1st Point of Aries	---	+102.9°	-23.9°	+95.1°
Earth True Anomaly (ν)	Earth Perihelion	-102.9°	---	-126.8°	+7.8°
Mars True Anomaly (ν)*	Mars Perihelion	+23.9°	+126.8°	---	-119°
Mars Solar Longitude (L_s)*	Mars Vernal Equinox	-95.1°	-7.8°	+119°	---

*Mars is inclined 1.85° to the ecliptic, rendering these conversions approximate and quasi-linear

The bottoms of the contour troughs on either side of the 180° ridge in the optimized porkchop plot is are not flat. They are lowest near the bridges and rise to a saddle on either side of the ridge somewhere in between the two bridges. Since most real transfers are not able to take place at the global optimum, it is useful to know when Type I is better than Type II, and vice versa. For Case 4, where the orbits are inclined but circular, the troughs are symmetrical about the ridge when sampled perpendicularly (see Figure 9a). However, when sampled on either side along the same Earth true anomaly they are not symmetric. Figure 9c shows the minimum ΔV's vs. Earth true anomaly for both Type I and Type II trajectories. The asymmetry along the true anomaly lines

cause the peaks between the bridges to be offset. This creates four regions – two regions where Type I is the best and two where Type II is the best. ΔV's vary from 5.6 – 7 km/s across all launch locations. Type I trajectories are preferred in the first 90 degrees after a nodal crossing.

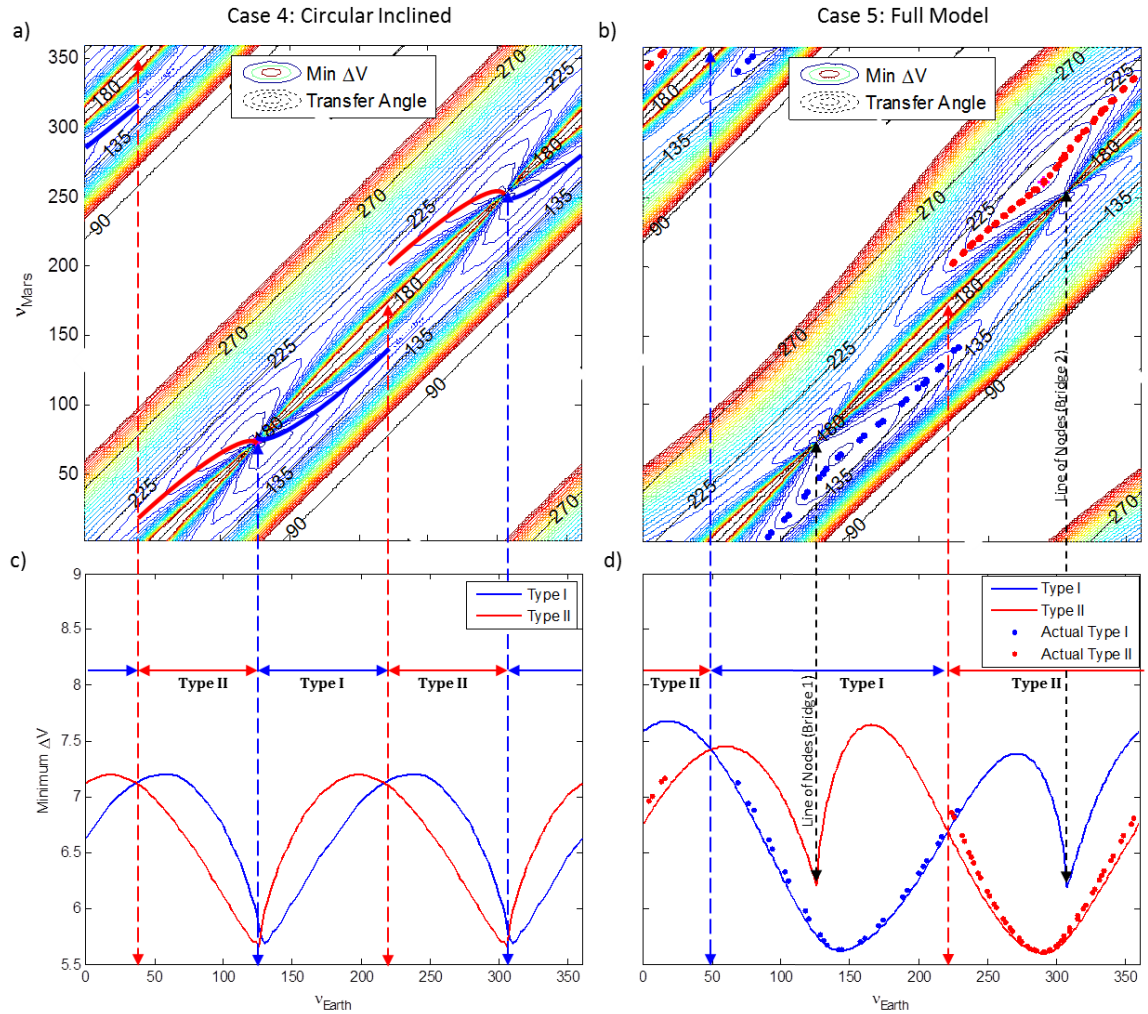

Figure 9. Regions of Type I vs. Type II optimality. Plots c) and d) show the minimum ΔV vs. Earth true anomaly for Cases 4 (circular inclined) and 5 (full model), respectively. Minima for both Type I and II are plotted. These plots indicate the regions where either type are more favorable. Actual data from ΔV optimized opportunities are plotted as points on Plots b) and d). Blue indicates Type I and red indicates Type II.

For the full model case in Figure 9b, the eccentricity of the orbits destroys the symmetry about the central ridge and pulls the minimum away from the bridges at the line of nodes. There are two large minima, one for each trajectory type. The magnitude of the total ΔV is driven by the three following factors in descending order from most dominant to least dominant:

1. Departure and arrival near the line of nodes
2. Arrival at the aphelion of the more eccentric body (Mars)
3. Departure from the perihelion of the less eccentric body (Earth)

The minimum ΔV transfer in each case are within 30 m/s of each other, but since Mars' perihelion is 74° from the ascending node and 116° from the descending node they are not symmetric and Type II is slightly more favored.*

The eccentricity of the orbits causes the local minimum near the bridges to move away from the line of nodes. This causes the bridges to no longer be switching points between trajectory type regions – reducing their number from four to two. As can be seen in Figure 9d, Type I trajectories are favored earlier in the year with Type II being favored later. The peaks at the switching points are also asymmetrical with the one at ν_{Earth} = 50° reaching 7.4 km/s and the one at ν_{Earth} = 230° reaching 6.7 km/s. Actual trajectory optima for the years 2011-2180 are plotted as data points. Note the absence of trajectories around the first switching point peak.

Comparison to Actual Data

It is possible to plot the actual ephemerides of Mars onto the optimized porkchop plot in terms of where Mars is with respect to Earth. Since the ratio of one Earth period to one Mars period is 365 days vs. 687 days, the slope on the n-n plot would be 365/687 = 0.53, or about ½, with some variation due to eccentricity. It would be more instructive to plot the location of Mars around 200-300 days in the future – roughly the length of optimal transfers. These isochrones would be parallel and cross the region of optimal transfer angles (the troughs on either side of the 180° transfer ridge, which has a slope of 1 on this plot) once every synodic period (~26 months). When the isochrones of the true ephemeris are equal to the optimal transfer times (of Figure 8b) for a given ν_{Earth}-ν_{Mars} pair, the transfer ΔV is equal to the optimal ΔV at that point.

Of course, the majority of the time the optimal transfer locations and transfer times will not exactly coincide. The regions where the actual transfer times and transfer locations approach those of the optimal porkchop plot then create the bi-lobed structure of the opportunity-specific porkchop plot. Actual porkchop plots for the Earth-Mars opportunities between 2011 and 2180 were created and the locations for optimized transfer ΔV were found. The data points are plotted on Figure 9b and Figure 9d, and the parameters up through 2073 are listed in Table 3. Note that they come quite close to the true minima, but not quite. It is also notable that the trajectories "avoid" the peak around ν_{Earth} = 20-70° and tend to be more dense around the global minimum Type II trajectory.

* The location of Earth perihelion also plays a role.

Table 3 - Optimal ΔV Transfers for 2011-2073

Year	ΔV_{Tot} km/s	ΔV_1 km/s	ΔV_2 km/s	ν_{Earth} deg.	ν_{Mars} deg.	Transfer days	T_{angle} deg.	Type	e	LD	AD
2011	5.70	2.99	2.70	303.1	278.5	307	208.6	2	0.210	11/9/2011	9/11/2012
2013	6.24	3.07	3.17	330.8	312.4	295	214.7	2	0.190	12/6/2013	9/27/2014
2016	7.12	3.36	3.76	13.1	354.0	277	214.1	2	0.176	1/17/2016	10/20/2016
2018	5.76	2.80	2.96	128.0	47.6	204	152.8	1	0.175	5/12/2018	12/2/2018
2020	6.32	3.71	2.61	199.2	112.6	205	146.5	1	0.231	7/25/2020	2/15/2021
2022	6.49	3.84	2.65	236.2	215.4	351	212.3	2	0.251	9/2/2022	8/19/2023
2024	5.82	3.36	2.45	265.9	242.0	334	209.3	2	0.237	10/2/2024	9/1/2025
2026	5.61	3.04	2.57	294.2	266.8	311	205.7	2	0.218	10/31/2026	9/7/2027
2028	5.99	3.02	2.97	318.8	298.8	301	213.2	2	0.198	11/24/2028	9/21/2029
2030	6.75	3.22	3.53	353.8	336.3	285	215.7	2	0.180	12/29/2030	10/10/2031
2033	6.33	3.00	3.33	102.8	17.4	198	147.8	1	0.167	4/16/2033	10/31/2033
2035	5.85	3.21	2.64	170.7	86.4	201	148.8	1	0.208	6/26/2035	1/13/2036
2037	6.85	4.03	2.82	223.8	203.3	354	212.7	2	0.254	8/20/2037	8/9/2038
2039	6.03	3.54	2.49	254.3	232.0	342	210.9	2	0.243	9/21/2039	8/28/2040
2041	5.62	3.13	2.48	283.3	256.5	319	206.3	2	0.226	10/20/2041	9/4/2042
2043	5.79	3.00	2.79	308.8	285.7	305	210.1	2	0.206	11/15/2043	9/15/2044
2045	6.41	3.11	3.30	338.7	320.9	292	215.4	2	0.186	12/14/2045	10/2/2046
2048	6.95	3.26	3.69	76.3	350.2	199	147.1	1	0.171	3/20/2048	10/5/2048
2050	5.63	2.83	2.80	141.2	62.4	206	154.4	1	0.185	5/26/2050	12/18/2050
2052	6.59	3.98	2.61	213.3	126.6	210	146.5	1	0.241	8/9/2052	3/7/2053
2054	6.31	3.73	2.58	242.7	221.3	348	211.9	2	0.248	9/9/2054	8/23/2055
2056	5.72	3.27	2.45	272.5	247.0	328	207.6	2	0.233	10/9/2056	9/2/2057
2058	5.65	3.01	2.64	298.9	272.6	308	207.0	2	0.214	11/5/2058	9/9/2059
2060	6.13	3.04	3.08	325.6	306.5	298	214.1	2	0.194	12/1/2060	9/25/2061
2063	6.95	3.29	3.66	3.7	345.8	281	215.4	2	0.178	1/8/2063	10/16/2063
2065	5.98	2.86	3.12	117.1	34.3	201	150.4	1	0.169	5/1/2065	11/18/2065
2067	6.10	3.49	2.61	187.6	101.1	202	146.7	1	0.222	7/14/2067	2/1/2068
2069	6.64	3.91	2.72	231.2	210.5	353	212.5	2	0.252	8/28/2069	8/16/2070
2071	5.90	3.44	2.46	260.8	237.3	337	209.7	2	0.239	9/28/2071	8/30/2072
2073	5.60	3.08	2.52	290.0	261.6	313	204.8	2	0.222	10/27/2073	9/5/2074

CONCLUSIONS AND FUTURE RESEARCH

The nature of Earth-Mars porkchop plot morphology and how it varies from opportunity to opportunity was investigated by the authors. Total transfer ΔV was used as a surrogate FOM that is used to optimize trajectories and to compare to actuals. The "best" trajectory of each opportunity varies from near-optimal up to 30% worse for the total ΔV FOM. The actual impact of these variances on interplanetary mission design is often a strong function of the mission objectives and propulsion technology. Orbiters utilizing chemical propulsion are most sensitive to the required ΔV both leaving Mars and upon arrival, although aeroassist techniques (aerobraking,

aerocapture) minimize the penalties associated with higher arrival velocities. Direct entry landed missions are typically much less sensitive to arrival velocity as long as constraints such as the maximum allowable heating rate and total heat load to their entry aeroshells can be maintained within the arrival conditions. Alternate FOMs should be investigated to determine the optimality of trajectories for different mission applications which may take into account things such as transfer time, launch declination, arrival date, entry speed, etc.

Earth-Mars geometry roughly repeats every 15 years, or 7 opportunities. However, the subtle differences in true anomalies amplify the effects of inclination, eccentricity, and transfer time, so as to make repeatability of most specific trajectory parameters crude at best and non-existent at worst, although "representative regions" of the porkchop plot coordinate space repeat from opportunity to opportunity. Applying constraints to these parameters to meet mission requirements further exacerbates the challenges of finding "exact repeats."

This type of comparative analysis across multiple launch opportunity has greatest utility during the earliest phases of planning for a mission or series of missions when programmatic uncertainties preclude detailed planning for a specific opportunity. Better understanding of the variability from opportunity to opportunity allows mission and system architects to better scope by how much the key mission-driven parameters of the system may vary depending on the selected opportunity, or, if programmatic robustness or flexibility to design a system capable of launching in more than one candidate launch opportunity is mandated, this type of analysis could prove invaluable.

Another pathway for future investigation is the opposite of mission specific applications of this research. Rather, it would be to further generalize the analyses presented in this paper to transfers between any two orbits. This would shed further light on the effects of orbital parameters on optimal transfers and the morphology of FOM contours. The key parameters of optimal transfers (ΔV_1, ΔV_2, locations, etc.) are derivable from e_1, e_2, Δi, and Γ. Much exists in the literature on numerical methods for trajectory optimization. However, it would be instructive to formalize analytically, visually, and algebraically the relationships between orbital parameters and optimal transfers.

ACKNOWLEDGMENTS

This research was carried out at the Jet Propulsion Laboratory, California Institute of Technology, under a contract with the National Aeronautics and Space Administration. Government sponsorship acknowledged.

REFERENCES

[1] A.B. Sergeyevsky, G.C. Snyder, and R.A. Cunniff, "Interplanetary Mission Design Handbook. Volume I, Part 2: Earth to Mars Ballistic Mission Opportunities, 1990-2005", JPL Publication 82-43, September 15, 1983.

[2] S. Matousek and A.B. Sergeyevsky, "To Mars and Back: 2002-2020. Ballistic Trajectory Data for the Mission Architect", AIAA 98-4396, AIAA/AAS Astrodynamics Specialist Conference, Boston, MA, August 10-12, 1998.

[3] L.E. George and L.D. Kos, "Interplanetary Mission Design Handbook: Earth-to-Mars Mission Opportunities and Mars-to-Earth Return Opportunities 2009-2024", NASA/TM-1998-208533, 1998.

[4] D.A. Vallado, *Fundamentals of Astrodynamics and Applications*, Space Technology Library, Microcosm Press, El Segundo, California, 2001.

[5] C.F. Capen, "A Guide to Observing Mars", *Strolling Astron*., Vol. 30, Nos. 9 - 10, p. 186 – 190, 1984.

[6] C.H. Won, "Fuel- or Time-Optimal Transfers Between Coplanar, Coaxial Ellipses Using Lambert's Theorem", *Journal of Guidance, Control, and Dynamics*, Vol. 22, No. 4, pp. 536-542, 1999.